

# Purification of A-Form DNA Fiber Samples by the Removal of B-Form DNA Residues

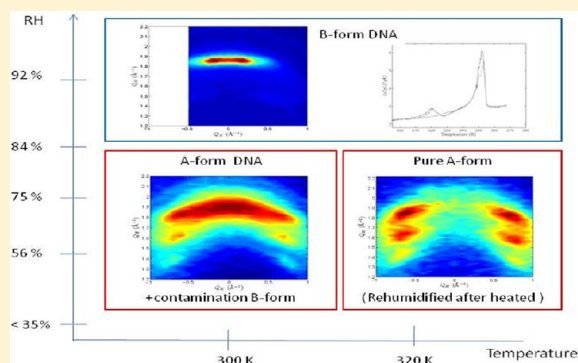
Jessica Valle-Orero,<sup>\*,†</sup> Andrew Wildes,<sup>†</sup> Jean-Luc Garden,<sup>‡</sup> and Michel Peyrard<sup>§</sup>

<sup>†</sup>Institut Laue Langevin, BP 156, 6, rue Jules Horowitz 38042 Grenoble Cedex 9, France

<sup>‡</sup>Institut Néel, CNRS - Université Joseph Fourier, 25 rue des Martyrs, BP 166, 38042 Grenoble cedex 9, France

<sup>§</sup>Laboratoire de Physique, Ecole Normale Supérieure de Lyon, 46 allée d'Italie, 69364 Lyon Cedex 07, France

**ABSTRACT:** To date, fiber diffraction on A-form NaDNA has always shown a B-form contamination. Here we have used optic microscopy, calorimetry, and neutron scattering techniques to define a method to obtain DNA fibres samples whose molecules are purely in the A-form. When the impure sample is heated to 320 K, the DNA molecules in the B-form undergo a transition into the A-form. Our studies have modified the accepted phase diagram for NaDNA films by including the dependence of temperature crucial for the purification of A-form samples by removal of B-form contamination.



## INTRODUCTION

The possibility of having samples of DNA molecules oriented in a fiber structure allowed Franklin and Wilkins to carry out the first structural studies of the molecule using X-ray diffraction.<sup>1,2</sup> The molecules assemble within the fiber in the form of a 1-D ordered structure, making DNA samples suitable for structural investigations. Base pair separation, unit cell dimensions, and structure can all be measured using scattering methods.

The conformational flexibility of fibers permits the DNA molecules to adopt different structures by changing the ionic nature and concentration of the solution or the hydration level of the molecules. The most common ones are the A- and B-forms. The molecules in these structures differ in the helix pitch and the number of nucleotides per pitch. On average, the DNA pitch extends to 28 Å with 11 base pairs for A-form and 34 Å with 10 base pairs for B-form. Furthermore, the organization of the cations and water within the DNA, which provides the stabilization of each of the structures, occurs differently. The A-form is stabilized by an organization of the cations and water molecules within the major groove of the double helix<sup>3</sup> and a more economic hydration of the phosphate groups.<sup>4</sup> As a consequence, the base pairs are tilted with respect to the molecular axis, resulting in a very compact structure. For the B-form, the hydration occurs in the minor groove. It is the most hydrated structure of all known conformations and is favored in solution. The base pairs stack perpendicular to the molecular axis.

The discovery of the DNA molecule in 1953<sup>5</sup> revealed the critical biological role of the molecule and rose biological questions about the rules governing genetic processes. It is now established that DNA functionality, and thus its interaction with

a biological particle, is highly dependent on sequence structure, but still today questions such as protein recognition and binding to DNA sequence<sup>6,7</sup> or mechanical properties of the molecule to allow bending around chromatin<sup>8</sup> and so on are under debate. Therefore, it is essential to understand the different DNA structures to be able to determine their biological application.

After the discovery of the DNA structure, the X-ray diffraction technique became the tool par excellence to study the effects responsible for DNA conformations in fibers.

The first characterization of the A- and B-forms presented clear features on their diffraction patterns. A strong Bragg peak associated with the spacing between base pairs along the fiber axis is observed for the B-form, and three off-axis Bragg peaks resulting from the tilt of the base pairs relative to the molecular axis are observed for the A-form.<sup>1</sup>

Later studies on these structures carried out by Brandes et al. in 1988 revealed that NaDNA fiber samples created under the optimal conditions to induce an A-form always contain some contribution of B-form.<sup>9</sup> This contribution is demonstrated by the presence of a broad Bragg peak along the fiber axis, which is characteristic of the B-form. Whereas Brandes et al. appear to be the first to acknowledge this effect, close observation of previous diffraction images from nominally "pure" A-form fiber DNA always show B-form contamination.<sup>10,11</sup> The transition of  $A \rightleftharpoons B$  has always been addressed in terms of the hydration of the sample. Within the literature it has been established that for NaDNA fiber samples the ranges of relative humidity (RH) at

Received: November 12, 2012

Revised: January 16, 2013

Published: January 18, 2013

room temperature to induce the corresponding DNA conformations are: around 40–88% RH for the A-form and >88% RH for B-form. In the case of fibers made with Li cations, A-form can never be adopted.

Within this observation of the B-contamination, further studies centered on the A-to-B transition in NaDNA solid samples were carried out by Brandes and coworkers using  $^2\text{H}$  solid-state NMR and X-ray fiber diffraction. They proposed several methods to eliminate the contamination of the B-form such as dehydration and addition of ethanol. However, they reduced rather than eliminated this contribution. There always appeared to be signs of disordered regions of B-form.

Binocular microscopy is also a powerful tool to probe the conformation of DNA via the length of the fiber. A reversible shortening of the fiber due to a B-to-A transition as a consequence of changes in the axial rise per base pair was reported by Zimmerman et al.,<sup>12,13</sup> driven by a decrease in the concentration of ethanol with respect to water in the fiber. Premilat et al. observed the same phenomenon with decreasing RH.<sup>14</sup>

More recent analysis in oriented fibres of NaDNA estimated a B-form contamination of  $\sim 10\%$  in A-form samples.<sup>15</sup>

In summary, it has become a challenge to have fiber samples with only an A-form configuration. The phase diagram in Figure 1 has been compiled by summarizing the humidity and counterion conditions from the literature.

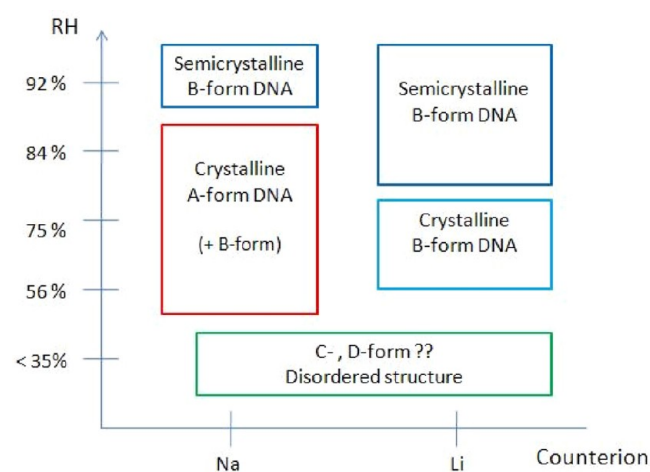


**Figure 1.** Phase diagram, relative humidity versus counterion, defining the different DNA forms.

As previously mentioned in the Introduction, DNA conformation plays a critical role in biological functionality. Much work has been accomplished on B-form DNA, and much less has been achieved on the A-form. However, studies carried out in the structure of a specific RNA polymerase showed that during the formation of the transcribed DNA-RNA chain this heteroduplex is in an A-form helix.<sup>16</sup>

We are presenting our studies on the effects of temperature on the macroscopic and microscopic properties of the samples and whether the detected changes could be attributed to the transition between B- to A-form DNA. Our studies consist of a strict characterization of samples of oriented DNA fibres using neutron diffraction, calorimetry, and optic microscopy techniques. Through these investigations we have determined a method for obtaining almost pure A-form NaDNA fiber samples using a heat treatment.

## EXPERIMENTAL METHODS

**Sample Preparation.** Samples made of oriented fibres of NaDNA from salmon testes were prepared using the wet spinning method.<sup>17</sup> These samples consist of films of oriented DNA fibres. To obtain samples in the B- and A-forms, the films were humidified under 92% RH and 56% RH respectively using an oversaturated salt solution of water. For those samples designated for neutron scattering measurements, deuterated water ( $D_2O$ ) was used to minimize the incoherent scattering. The methods of the preparation of the samples for the different purposes, differential scanning calorimetry (DSC) and neutron scattering measurements, have been described elsewhere.<sup>18–20</sup>

For all measurements the samples were sealed within a sample cassette to maintain fixed the number of water molecules throughout the experiments. Subjecting the samples to changes in the temperature results in changes in the dew point and thus the RH, but the available number of water molecules stayed constant.

**Differential Scanning Calorimetry.** DSC measurements were carried out using a Setaram Micro DSC III. The initial conditions of the films, ionicity content and concentration of the ethanol during the spinning process, were the same for all of our samples. The films weighed around 100 mg. An A-form film was cut into two equal pieces, whereas for the B-form an entire film was used. For every measurement, a film was rolled up and placed in an Hastelloy sample tube that was sealed to conserve the water content. The measurements were made relative to a reference tube that was left empty.

The samples were thermalized in the DSC at 293 K and then cooled to 278 K. The B-form film and one of the pieces of the A-form sample were first heated from 278 to 368 K and to 383 K, respectively, whereas the ramps were recorded as a DSC scan. At the maximum temperature, the samples were kept for 10 min and then cooled back to 278 K. The heating–cooling ramps were performed at a scanning rate of 0.6 K/min. For the second piece of the A-form film, a first temperature ramp was performed from 278 K to 321 K, cooled to 278 K, and subsequently heated up to 368 K.

Each of the measurements was recorded in the form of differential heat flux  $\Delta P$  as a function of temperature. Due to an intrinsic delayed response of the instrument to a change of temperature, the heat flux was corrected from an instrument response defined as  $\tau$ , given by the supplier as 60 s. The specific heat  $\Delta C$  is directly related to the heat flux by the following formula

$$\Delta C = \left( \Delta P + \tau \frac{d\Delta P}{dt} \right) \cdot \left( \frac{dT}{dt} \right)^{-1} \quad (1)$$

where  $(dT/dt)$  is the scanning rate,  $T$  is temperature and  $t$  is time.

**Optic Microscopy.** These measurements were carried out on as-spun films of A-form. Each sample corresponded to a  $2 \times 2$  cm<sup>2</sup> piece of a NaDNA film. The film was exposed to 56% RH for 3 days prior to the optic microscopy measurements. Each sample was extracted from its humidity chamber and placed between two glass plates, then sealed with adhesive tape to preserve the hydration. The ensemble was then placed on a copper base. The temperature was increased at a rate of 5 K/min. The macroscopic thermal behavior of the film was recorded, whereas photographs were taken every 10 K.

**Neutron Scattering.** The samples were placed in a thin niobium envelope, and then inside an aluminum cassette which was sealed using a lead wire joint.

The characterization of the different DNA structures via neutron diffraction took place on the three-axis spectrometers IN3 and IN8 at the Institut Laue-Langevin. Both IN3 and IN8 were configured with a pyrolytic graphite (PG) monochromator. A PG analyzer was used on IN3, whereas no analyzer was used on IN8. For both instruments, the wavelengths were set to 2.36 Å, and the  $Q$ -resolution was defined by 40' collimators before and after the sample. A PG filter was also placed before the sample to remove higher order wavelengths.

Two sample orientations were investigated. To explore the reciprocal space along the molecule and thus correlations along that direction, we aligned the samples with the fiber axis in the scattering plane. This orientation is hereafter defined as longitudinal. For the second orientation, the samples were rotated 90° so that the fiber axis was perpendicular to the scattering plane. This orientation is hereafter referred to as transversal. These measurements aimed to probe Bragg peaks in the reciprocal space transverse to the fiber axis to establish any correlation between the DNA molecules within the fiber. The DNA reciprocal system,  $(Q_H, Q_K, Q_L)$ , has been defined in Figure 2, where the fiber axis was conventionally defined to be along the  $Q_H$  axis.

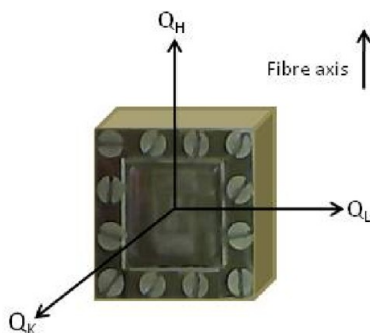


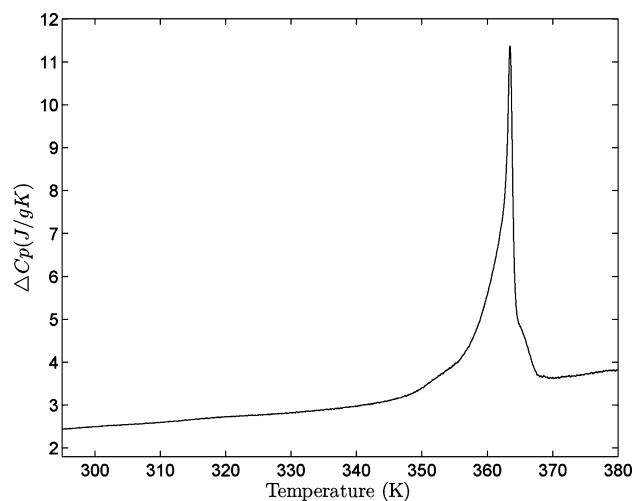
**Figure 2.** Schematic of the DNA fiber sample inside the aluminum sample holder. The DNA reciprocal coordinate system with respect to the sample cassette has been represented.

Longitudinal and transverse reciprocal space maps (RSMs) were measured for both B- and A-form as-spun samples at room temperature. The A-form sample was then aligned in longitudinal orientation inside a cryofurnace, and measurements were taken along  $Q_H$  (fiber axis) as a function of temperature from 295 to 324 K. The measurements were centered at the position of the residual B-form Bragg peak. The sample was then cooled to room temperature, removed from the cassette, and left in a desiccator with 56% RH to rehumidify for 1 week before measuring the RSM again.

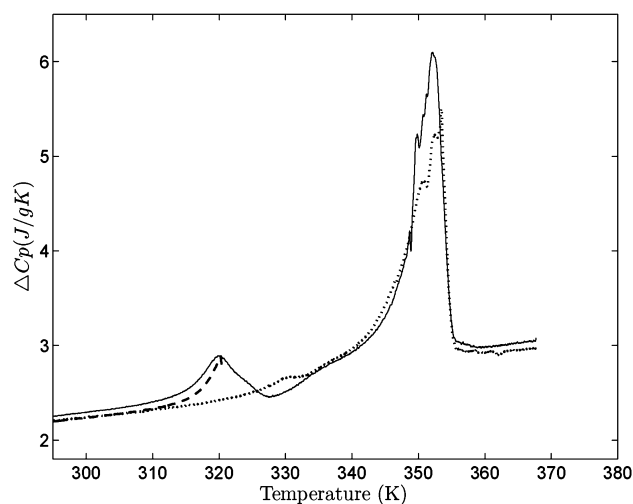
## RESULTS

**Calorimetry.** The melting profiles of as-spun films prepared in the different DNA conformations are shown in Figure 3a,b. The curves present heat capacity as a function of temperature. They exhibit a large peak at  $T > 350$  K, which can be assigned to the denaturing of the DNA molecules in which the base pairs break with increasing temperature.

The melting profile of a B-form fiber sample is shown in Figure 3a and is consistent with our previous measurements.<sup>18,19</sup> As expected, the direct DSC heating ramp shows



(a) B-form



(b) A-form

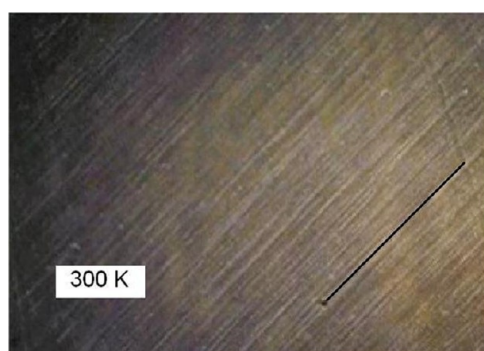
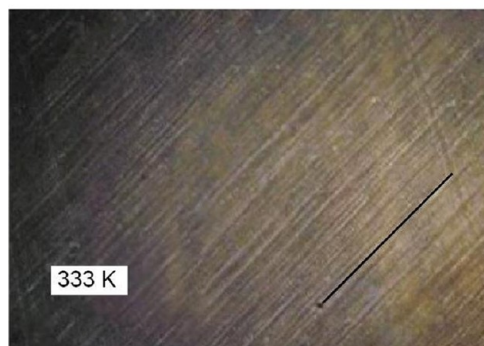
**Figure 3.** DSC heating ramp of different DNA conformations. Panel a corresponds to a direct heating ramp of a B-form sample. Panel b corresponds to the curves of two pieces of the same A-form sample humidified under 56% RH. Sample 1 was heated from 278 to 368 K directly (solid line) (two transitions are visible), whereas sample 2 went through a preheating process from 278 to 318 K (dashed line), was cooled, then was heated again to 368 K (dotted line). The dashed curve shows an indication of the low-temperature transition associated with a configurational transition, whereas in the dotted curve only the highest temperature transition is visible.

one endothermic transition, which we associate with DNA denaturing because it occurs in the temperature range in which the transition is observed in solution. These samples show a smooth heat capacity, suggesting configurational stability until the melting temperature is reached at ~360 K.

When a sample in an A-form is heated from 278 to 368 K, the DSC ramp shows two endothermic transitions, as shown in Figure 3b (solid line). The transition at ~351 K is due to the melting transition of the DNA. The first transition occurring at 318 K does not appear in B-form samples, which have a single and stable molecular configuration. A second experiment was then carried out with another piece of the same A-form film as previous measurements. The data are also shown in Figure 3b. On heating the sample to 321 K (dashed line), the ramp shows signs of a transition. The sample was then cooled, and a second

heating ramp from 278 to 368 K was performed (dotted line). The subsequent heating scan shows only the transition at the highest temperature. The transition at  $\sim 320$  K is suppressed, implying that the sample remained thermally stable until it reached the melting transition. We believe that the first transition is due to the B-form impurities being converted to A-form, and this is confirmed by the results presented in the following sections.

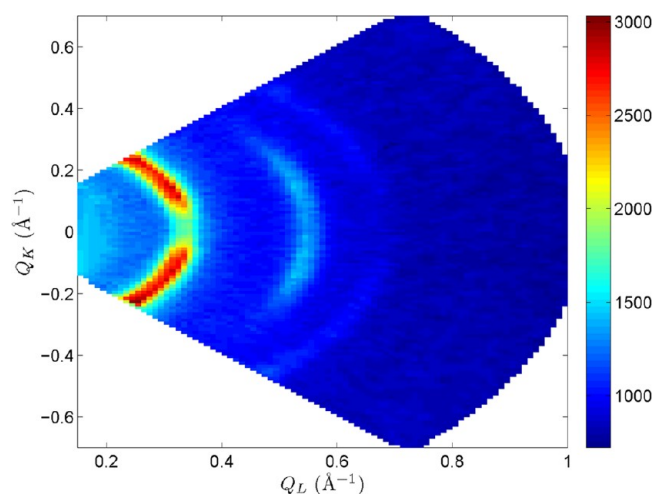
**Optic Microscopy.** Figure 4 shows the optical observation of the fiber structure of the DNA sample taken at room

(a)  $T = 300$  K(b)  $T = 333$  K

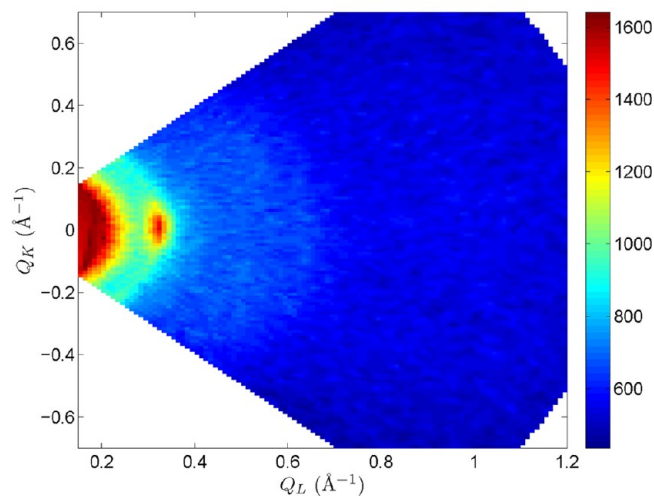
temperature 300 K (a) and at 333 K (b). The fiber orientation is clearly visible from the texture of the images. A black line is drawn to represent the distance between two artifacts detected on the film. When the temperature of the sample was increased, a collective shortening of the fibres was visible at  $\sim 328$  K. From Figure 4b, the black line joining the two artifacts appears to have shortened by 7% with respect to that drawn on the image taken at room temperature. As described in the Introduction, there is a direct relation between the length of the DNA molecules and the length of the fiber,<sup>14</sup> and thus these measurements are a hint that heating the film to 333 K induces a B-to-A transition.

**Neutron Scattering. Sample Characterization of As-Spun Films.** Before discussing the points relevant for the B- to A-form transition, we would like to point out an interesting feature concerning the state of the fiber. When measuring in the  $Q_K$ - $Q_L$  reciprocal space, features are found in both

conformations. These give insight into the transverse structural properties of the samples, related to the intermolecular correlations of the DNA molecules within the fiber. The reason of the orientation of molecules between fibres may be associated with a macroscopic shape of the actual fiber, giving rise to some sort of self-organization of the fibers with their neighbors. Figure 5 shows in more detail the RSM of A- and B-forms in the transversal orientation.



(a) B-form



(b) A-form

**Figure 5.** (a) B-form transversal Bragg peak and (b) A-form transversal Bragg peak.

A more complete description of the reciprocal space in 3-D of as-spun samples of oriented DNA fibres is shown in Figure 6. After their preparation the samples were exposed to the optimal humidity conditions to induce A- and B-forms. The RSMs were measured at room temperature.

In the process of the sample preparation using the wet-spinning apparatus,<sup>21</sup> the DNA fiber is wound around a cylinder like a thread around a bobbin. Naively one might think that during the process all of the fibers are collinear, but they will be randomly rotated around their cylindrical axis with respect to their neighbors. In reciprocal space, this will lead to a cylindrically averaged intensity of the Bragg peaks in the  $Q_K$ -

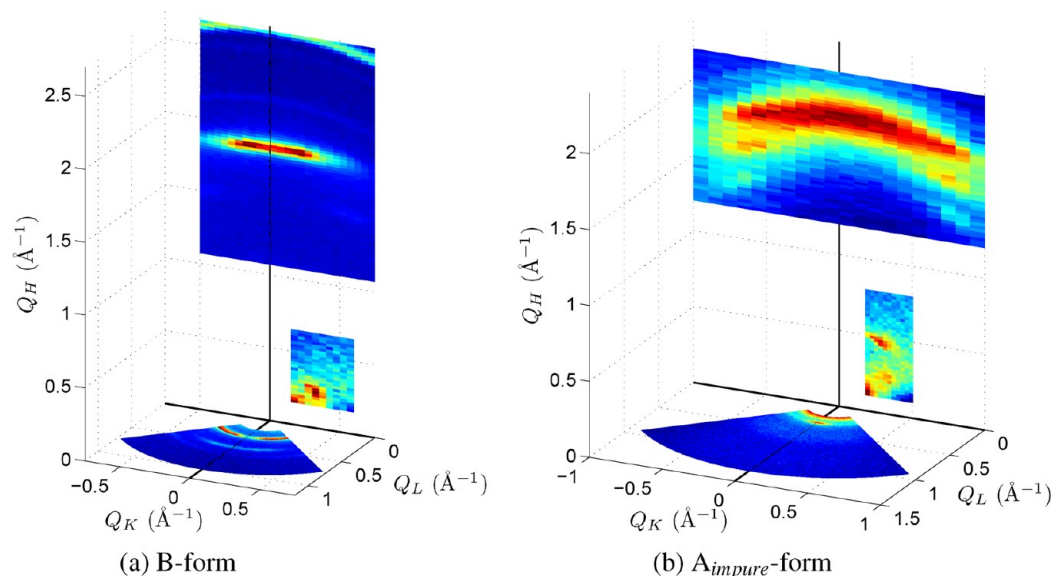


**Figure 6.** Reciprocal space maps obtained in the  $Q_H$ - $Q_K$  plane and  $Q_K$ - $Q_L$  plane for a spun DNA fiber sample in both B-form (a) and  $A_{\text{impure}}$ -form (b). Maps were plotted in a 3-D coordinate system.

$Q_L$  plane, that is, “powder rings”. The observed features have structure in their intensities, indicating that they are not powder-like. This was a surprising result because it revealed that not only are the molecules oriented within a fiber but also they are oriented between fibres. This perpendicular order is stronger for the A-form than for the B-form.

From the B-form diagram, one can see the intense Bragg peak in the  $Q_H$ - $Q_K$  centered at  $(1.87,0) \text{ \AA}^{-1}$ . There is also a low- $Q$  Bragg peak at  $(0.25,0.3) \text{ \AA}^{-1}$ . In the case of the A-form samples, the RSM in the  $Q_H$ - $Q_K$  plane shows the three off-axis peaks, displayed along the molecular axis at  $Q_K = \pm 0.7 \text{ \AA}^{-1}$ . A Bragg peak at  $(1.87,0)$  associated with the B-form contamination is extremely conspicuous. In the low- $Q$  part of the reciprocal space, there is an intense peak at  $(0.45,0.25) \text{ \AA}^{-1}$  from the A-form, and a less intense peak at the same position as in the B-form  $(0.25,0.3) \text{ \AA}^{-1}$ , again a consequence of B-form contamination.

**Temperature Dependence.**  $Q_H$  scans of impure A-form samples centered at the expected position of a B-form Bragg peak were taken at different temperatures, from 295 to 324 K. The scans were fitted with Lorentzian functions keeping all parameters free. Figure 7 shows the fitted scans for different temperatures. This Figure gives a better appreciation of the temperature dependence of the B-form Bragg peak and thus the transition temperature. We can conclude that a thermally induced transition marked by a drop of the intensity of the Bragg peak of the B-form occurs around 318 K.

Figure 8 shows the RSM in the  $Q_H$ - $Q_K$  plane of the spun A-form sample measured at two different temperatures, 300 and 320 K. The RSM includes the B-form contamination Bragg peak and the three off-axis Bragg peaks at positive  $Q_K$ . The comparison between both contour plots shows a collective broadening of the peaks and a decrease in the intensity, as seen in the individual scans. This effect can be explained by a global disordering of the crystalline fiber structure.

The samples were heated at 320 K and left for 8 h. This temperature was chosen based on our calorimetric results shown in Figure 3b, where the peak of the first transition in impure A-form samples was centered at  $\sim 320$  K. Moreover, this temperature is also consistent with that at which the fiber

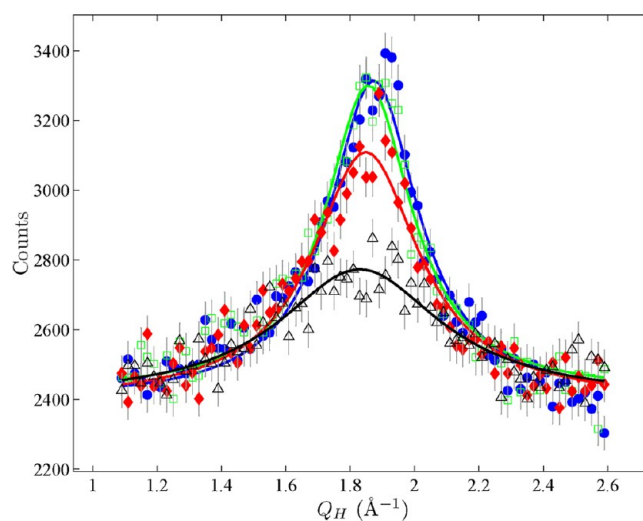


**Figure 7.** Scans centered at the residual B-form Bragg peak in an A-form DNA sample taken at different temperatures: 295 (circles), 311 (open squares), 319 (diamonds), and 324 K (open triangles). The data were fitted with Lorentzian functions.

shortening was observed with optic microscopy. After that, they were cooled and rehumidified to 56% RH, this being the nominal humidity needed for an A conformation. The RSM of the samples was then measured. Figure 9b,c shows, respectively, the RSM of the as-spun fiber in A-form with B-form contamination and that of the heat-treated fiber. For comparison, the RSM of a B-form sample is also presented in Figure 9a.

Figure 9c shows that the low- $Q$  feature associated with the B-form Bragg peak at  $(0.25,0.3) \text{ \AA}^{-1}$  has practically disappeared in the heat-treated sample, whereas the A-form Bragg peak at  $(0.5,0.25) \text{ \AA}^{-1}$  appears even more localized and intense. A similar effect is detected in the high- $Q$  region in the reciprocal space, where there are no traces of B-form Bragg peak, and the three-off axis peaks are strongly distinguishable. Thus, the images demonstrate that the structure of the heat-treated sample is very close to a pure A-form. We believe that a more

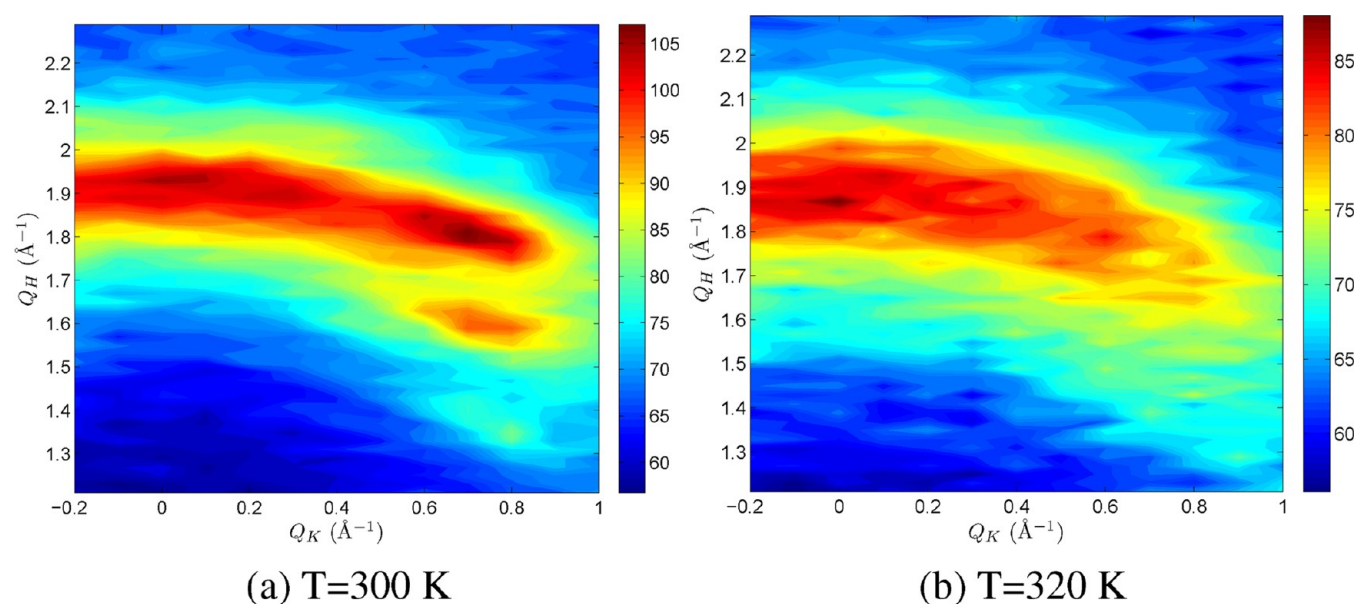


**Figure 8.** High- $Q$  reciprocal space maps of the impure A-form measured at 300 (a) and 320 K (b).

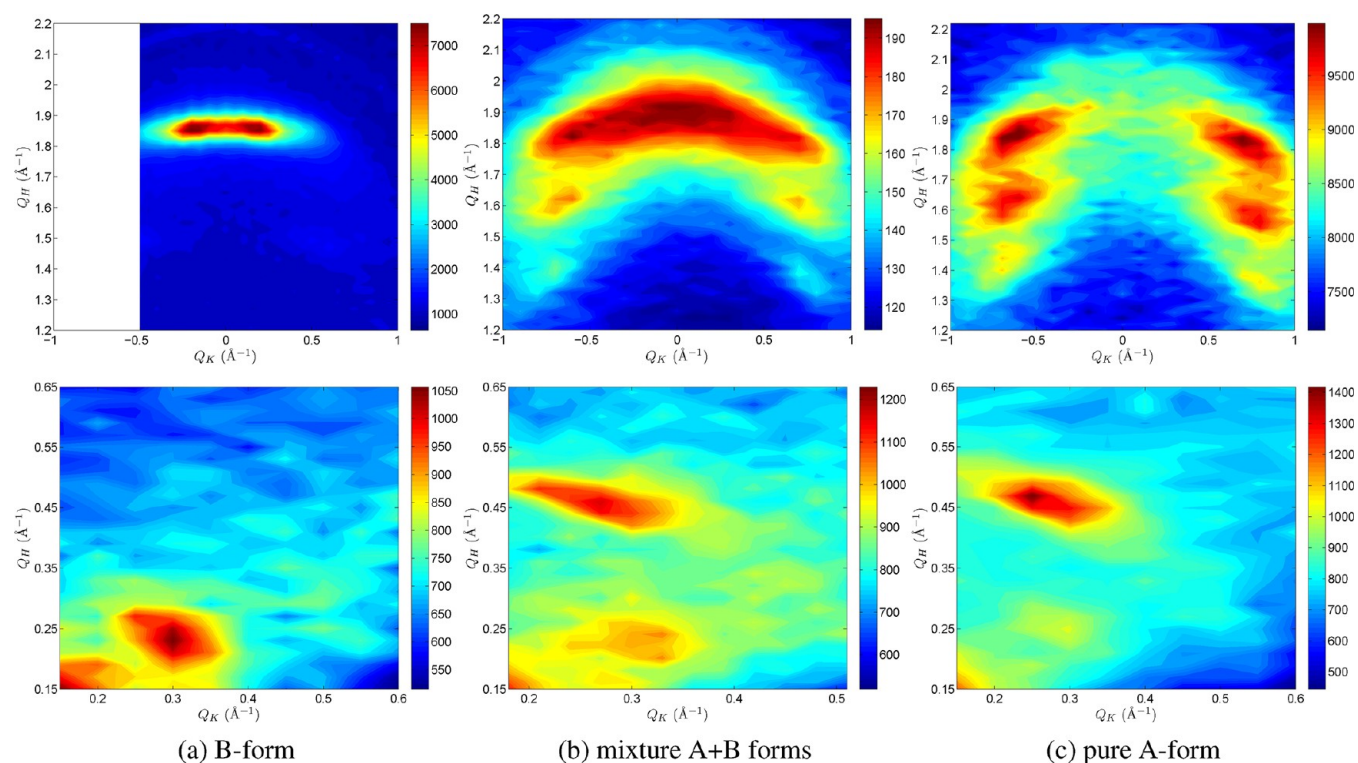


**Figure 9.** RSM in the  $Q_H$ - $Q_K$  plane of the B-form (a), impure A-form (b), and purified A-form (c). All measurements were made at 300 K.

careful heat treatment to slightly higher temperatures will suppress all B-form contamination.

## DISCUSSION

The combination of neutron scattering, calorimetry and optic microscopy has provided the global picture that heat treatment can significantly suppress B-form contamination in A-form fiber NaDNA. This is the key to a purification method for A-form DNA samples.

The low-temperature peak at  $\sim 320$  K in the DSC signal was previously observed and discussed by Lee and coworkers as an

endothermic process due to the loss of ordered structure driven by dehydration.<sup>22</sup> We believe that when an impure A-form sample is heated above 320 K, the higher hydrated residual B-form segments present within the sample start to rearrange into the A-form by releasing the additional water molecules to the surroundings.

Our optical observations are consistent with the conformational transition between B and A that was previously observed by Premilat et al. with physicochemical experiments in the form of a decrease in the fiber dimensions, diameter, and length as the temperature increases due to the loss of hydration.<sup>23</sup> This is expected because the molecules take an A-form in the lower

hydrated system, compacting themselves to fill the space the water has left. Because the A-form of the molecule is shorter than the B-form, the B-to-A transition is accompanied by a distortion of the fiber structure, as seen by optic microscopy. Moreover, the optical transition appears within the same temperature window as the endothermic peak observed in calorimetry, reinforcing our hypothesis of a conformational change.

The length of the fiber containing a coexistence of A+B forms was previously calculated by Premilat using the following relation<sup>14</sup>

$$L_{A+B} = X_B L_B + X_A L_A \quad (2)$$

where  $X_B$  and  $X_A$  correspond to the fractions of nucleotides in conformations B and A, respectively. From our optic microscopy images, we determined that the fiber length in a A+B state decreased by 7% when it underwent the transition at 320 K, becoming A-form. Applying the same formula gives an estimation of the percentage of B-form contamination within our as-spun A-form fiber sample. By solving the following equations

$$L_{A+B} = \frac{100}{93} L_A \quad (3)$$

and

$$L_{A+B} = X_A L_A + X_B L_B \quad (4)$$

$$\text{for } X_A + X_B = 1$$

and using the values given in Table 1 in ref 14,  $L_A$  (66% RH, A pure) = 2.875 and  $L_B$  (95% RH, B pure) = 3.775; the percentage of nucleotides of each conformation ( $X_A$  and  $X_B$ ) is 76% and 24% for A- and B-forms, respectively.

In the case of a diffraction experiment, the transition is also observed by the loss of the intensity of the Bragg peaks from the B-form. However, the complete structure and orientation of the DNA fibres is not lost, and this is why an ordered and oriented sample can be recovered after a sufficiently long relaxation and proper rehumidification at room temperature. The proper rehydration of the sample to favor an A-form provides what we call a "pure A-form", whose structure is stable up to melting temperatures. This is an important step toward further studies of DNA in its A-form without the perturbation due to B contamination.

When the sample was cooled to 278 K in the calorimetry experiment after heating to 318 K, we expected there to be no remains of the B-form, and hence an endothermic peak associated with B to A transition was scarcely observed in the second DSC heating scan. Rehumidification was not needed for this experiment because this technique is not sensitive to the periodic structure.

Figure 1 shows the phase diagram of the A- and B-forms of DNA that was generally accepted before our study. What was missing on this phase diagram is a temperature axis, crucial for obtaining pure A-form samples. We have shown that if one increases the temperature to 320 K, then the B-contamination in impure A-form converts to pure A. As a result, the phase diagram in Figure 1 was modified to give Figure 10. The area marked A is indeed pure A-form.

Regarding the analysis of the transversal orientation of the sample, we showed that the Bragg peaks are not powder rings because their intensities are not cylindrically constant, although they do have strong texture or preferred orientation.

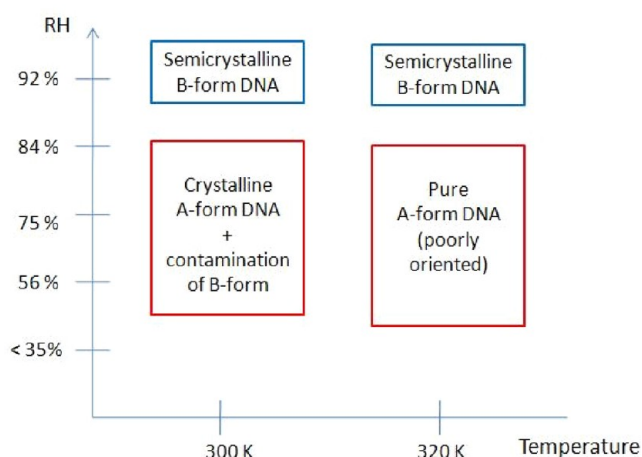


**Figure 10.** Corrected phase diagram for NaDNA films with relative humidity as a function of temperature. Pure A-form in the fiber samples can be achieved by increasing the temperature to 320 K as a result the fiber structure loses part of its orientation, which can be then recovered by rehydrating the sample. Because we have not studied possible other forms of DNA, such as the C-form, we have not indicated them on this diagram.

## CONCLUSIONS

We have carried out investigations to characterize the structure of oriented DNA fibres in the A- and B-forms. The studies were carried out using neutron diffraction, optic microscopy, and calorimetry. The contamination of B-form in A-form NaDNA fiber samples is always present. We found a simple method that allowed us to obtain almost pure A-form samples crucial for future studies in the investigation of the melting transition of this conformation compared with those carried out in the B-form.<sup>18</sup>

Neutron diffraction measurements made in the B-form Bragg peak of an A-form sample as a function of temperature showed that the intensity dropped considerably around 320 K until the extinction of the peak around 325 K. A subsequent rehumidification of the sample under 56% RH showed that the A-form features were recovered, and almost no traces from the B-form were present. This transition corresponded to the small endothermic peak observed with calorimetry and a shortening of the fibres as seen by optic microscopy and is consistent with a redistribution of water within the fiber. Therefore, our studies lead us to the determination of a method to obtain pure and stable A-form samples by the removal of B-form contamination and hence to redefine the accepted phase diagram to include the temperature dependence on the DNA forms.

## AUTHOR INFORMATION

### Corresponding Author

\*E-mail: valleorero@ill.fr.

### Notes

The authors declare no competing financial interest.

## ACKNOWLEDGMENTS

We thank Emmanuel André from Pôle de Capteurs Thermométriques et Calorimétrie for his support in the realization of the optical microscopy observations. The allocation of beam time by the ILL and the aid of the IN8 and IN3 instrument teams are gratefully acknowledged. We

also thank S. Helmut and M. Johnson for their financial support.

## ■ REFERENCES

- (1) Franklin, R.; Gosling, R. G. *Acta Crystallogr.* **1953**, *6*, 673–677.
- (2) Wilkins, M. H. F.; Stokes, R.; Wilson, R. *Nature* **1953**, *171*, 738–740.
- (3) Fuller, W.; Pope, L. H. *Biophys. Chem.* **1998**, *70*, 161–172.
- (4) Grimm, H.; Rupprecht, A. *Physica B* **1991**, *174*, 291–299.
- (5) Watson, J.; Crick, F. *Nature* **1953**, *171*, 737–738.
- (6) Seeman, N. C.; Rosenberg, J. M.; Rich, A. *Proc. Natl. Acad. Sci. U.S.A.* **1976**, *73*, 804–808.
- (7) Dostál, L.; Chen, C. Y.; Wang, A.; Welfle, H. *Biochemistry* **2004**, *43*, 9600–9609.
- (8) Dickerson, R. E.; Drew, H.; Conner, B. N.; Wing, R. M.; Fratini, A. V.; Kopka, M. L. *Proc. Natl. Acad. Sci. U.S.A.* **1982**, *216*, 475–485.
- (9) Brandes, R.; Voldand, R.; Keans, D. R. *Biopolymers* **1988**, *27*, 1159–1170.
- (10) W. Fuller, H. R. W.; Wilkins, M. H. F.; Hamilton, L. D. *J. Mol. Biol.* **1965**, *12*, 60–80.
- (11) Fuller, W.; Forsyth, T.; Mahendrasingam, A. *Philos. Trans. R. Soc., B* **2004**, *359*, 1237.
- (12) Zimmerman, S.; Pfeiffer, B. *J. Mol. Biol.* **1979**, *135*, 1023–1027.
- (13) Zimmerman, S.; Pfeiffer, B. H. *J. Mol. Biol.* **1980**, *142*, 315–330.
- (14) Premilat, S.; Harmouchi, M.; Albiser, G. *Biophys. Chem.* **1990**, *35*, 37–45.
- (15) Krisch, M.; Mermet, A.; Grimm, H.; Forsyth, V.; Rupprecht, A. *Phys. Rev. E* **2006**, *73*.
- (16) Graham, M. T.; Cheetham; Thomas, A. S. *Science* **1999**, *286*, 2305–2309.
- (17) Rupprecht, A. *Biochim. Biophys. Acta* **1970**, *199*, 277–280.
- (18) Wildes, A.; Theodorakopoulos, N.; Valle-Orero, J.; Cuesta-López, S.; Garden, J.-L.; Peyrard, M. *Phys. Rev. Lett.* **2011**, *106*, 048101.
- (19) Wildes, A.; Theodorakopoulos, N.; Valle-Orero, J.; Cuesta-López, S.; Garden, J.-L.; Peyrard, M. *Phys. Rev. E* **2011**, *83*, 061923.
- (20) Valle-Orero, J.; Garden, J.-L.; Richard, J.; Wildes, A.; Peyrard, M. *J. Phys. Chem. B* **2012**, *116*, 4394–4402.
- (21) Rupprecht, A. *Acta Chem. Scand.* **1966**, *20*, 494–504.
- (22) Lee, S.; Debenedetti, P.; Errington, J.; Pethica, B.; Moore, D. J. *Phys. Chem. B* **2004**, *108*, 3098–3106.
- (23) Premilat, S.; Albiser, G. *C. R. Acad. Sci., Ser. III* **1995**, *318*, 553–557.